

Simulation of ionic water solutions and verification of the Jones-Dole relation.

Author: Joan Mañas Martínez

Facultat de Física, Universitat de Barcelona, Diagonal 645, 08028 Barcelona, Spain.*

Advisor: Giancarlo Franzese

(Dated: June 2nd, 2016)

Abstract: Despite the diffusion anomalies of water ionic solutions have been widely studied in recent years, a complete connection between them and the nature of the intermolecular interaction of water and ions is still lacking. In this work, we hypothesise a mean-field like specific form for the influence of the concentration on the hydrogen bond energy. We find that the diffusivity vs concentration curves follow the empirical Jones-Dole expression over regions of the phase diagram where the diffusion anomaly is present.

I. INTRODUCTION

A. Relation of water diffusion anomaly with HB formation

Liquid water unique properties are related to the nature of hydrogen bonds (HB) between H_2O molecules (see fig. 1). For most liquids at given temperature, density increases with pressure along isotherms. While for bulk water it is true above a certain temperature, for isotherms below this temperature there is a pressure range in which density decreases with increasing pressure (i.e. water expands when compressed). This implies a density local maxima and minima along isotherms, and is called the water density anomaly. In a similar way, while above a certain temperature water diffusivity behaves as we would expect for a normal liquid (i.e. decreases with increasing pressure), it shows an anomaly inside a certain range, with a diffusion minima and maxima along isotherms. The origin of these and many more (at least 64) anomalies of water has been widely discussed. A somewhat intuitive explanation can help us to understand ([1], [2]). At low P the minimum energy HB structure is a tetrahedral ordination of molecules, which is present in Ih ice (fig. 2). The most remarkable feature of

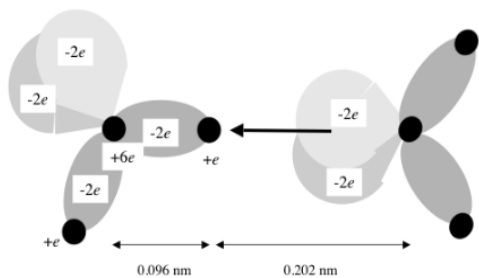


Figure 1: Schematic representation of the hydrogen bond between two water molecules. Extracted from [1].

this structure is being 'full of voids', implying an increase of volume per molecule. In liquid water the structure is more disordered because of thermal agitation, with water molecules moving randomly through available space.

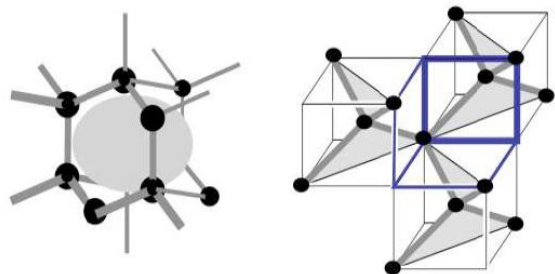


Figure 2: Right: Schematic representation of the HB network with the empty space emphasized in gray. Right: Schematic representation of the tetrahedral HB network. Extracted from [1].

This increases the probability for water molecules to be, in average, more closer among them: positions are more equiprobable to be occupied by a molecule, and water behaves as a normal liquid. For lower temperatures, liquid water retains a structure that resembles more to the Ih ice one, due to the smaller influence of thermal agitation. When pressure is decreased below a certain point, molecules are more likely to be bounded in the HB network positions, while when it is increased above this point, it forces HBs to break, giving rise to an increase of diffusivity. In ref. [3] it has been shown that, actually, the diffusivity minima coincides with the density maxima for a given isotherm, which indicates the close relation of these anomalies with the nature HB formation.

This intuitive explanation is a good simplification since recent works on water simulations (ref. [4] and [5]) have shown that, simulation models that ignore intermolecular cooperative interactions but introduce a systematic coupling between HB formation and volume increase, do actually reproduce density and diffusion anomalies.

*Electronic address: joanmanasm@gmail.com

B. Ionic solutes and its relation with HB formation

HB water network is perturbed by ions, modifying water thermodynamic behaviour. Traditionally, as mentioned in ref. [6], there has been an empirical distinction of two kinds of solutes in water, depending on the sign of the coefficient (B) in the following Jones-Dole equation for the relative viscosity of the solution:

$$\frac{\eta}{\eta_w} = 1 + A \cdot c^{1/2} + B \cdot c \quad (1)$$

Thus, solutions with positive B are told to be *structure makers* and those with negative B are told to be *structure breakers*. Traditionally it has been attempted to connect the structure makers and breakers distinction as an effect of ions to enhance or undermine structural HB network features. However, structural data from neutron diffraction studies ([6]) has shown, recently, that the perturbation due to ions can be seen as a clear change in the oxygen-oxygen water correlation function. The most important conclusion from this, is that the effect of ions in water extends far beyond the molecules in the ions solvation shells. Instead, the presence of ions can be seen as a global change in the correlations among water molecules. Moreover, in ref. [6] it has been shown, in one hand, that the presence of solutes in water affects the percolating clusters of the HB network in the same way, independently of being structure breakers or makers: enhancing or decreasing viscosity can not be linked to enhancing or decreasing the HB structure. On the other hand, the same work has shown that the viscosity of the solution with respect to pure water, can be related to the difference between oxygen-oxygen distance in pure water and ion-oxygen distance in the solution: the sign of this difference determines whether we are talking about structure makers or breakers.

Another important work supporting the effect of ions in water far beyond the first solvation shell is ref. [7]. On this work, charge transfer between ions and water molecules is taken into account through molecular dynamics simulations, in good agreement with experimental data. More precisely, it shows that the presence of ions is reflected among water molecules far beyond ionic immediate vicinity through non-local quantum mechanical effect of electrons.

C. Our hypothesis

In this work we reproduce the effect of ion concentration on the diffusivity assuming a non-local effect of the ions on the HB interactions. We use the knowledge that the presence of ions is weakening the HB interaction. If E_0 is the HB bonding energy when the ion concentration is $c = 0$, general considerations [6, 7] tells us that $E(c) < E_0$ for $c > 0$, i.e. $E(c)$ has a maximum $E = E_0$

for $c = 0$. Hence for small enough c we can assume that

$$E(c) = E_0 - \frac{1}{\beta} c^2. \quad (2)$$

In the following we will consider a water model in which the HB interaction is represented as the sum of two terms. The first is pair-additive and represents the directional part of the HB between two molecules and has a characteristic energy J_w in bulk water. The second represent the many-body part of the HB, involving the first hydration shell of each molecule, with a characteristic energy J_σ . We assume that the eq. (2) for this model implies that the pair-additive component of the HB has an energy that changes with c as

$$J(c) = J_w - \frac{1}{\beta} c^2. \quad (3)$$

This relation implies that

$$c \propto \sqrt{J_w - J}. \quad (4)$$

In water it is known that at ambient conditions and in a wide range of temperatures T and pressures P the diffusion constant and viscosity are related by the relation $D \propto 1/\eta$. Hence we can rewrite the Jones-Dole relation eq. (1) as

$$D^{-1} = D_w^{-1} + A' \cdot (J_w - J) + B' \cdot (J_w - J)^2. \quad (5)$$

In the following we perform Monte-Carlo simulations for a many-body model of a water monolayer in a wide range of P and T to verify the validity of the above relation.

II. MODEL AND SIMULATIONS

A. Many-body water model

We adopt the many-body model for a water nanoconfined monolayer of ref. [4]. This model

- Describes a water monolayer of a total volume V confined between two hydrophobic walls separated by a distance $h = 0.5$ nm, with double periodic conditions, that can be represented by its projection in 2 dimension.
- It consists of N water molecules distributed among M square cells ($M > N$), each with a volume $v = V/M$. Each cell contains one molecule at most.

In this model, interactions among particles are reproduced through four contributions to the total free energy of the system: (i) a dispersive van der Waals isotropic interaction contribution H_{LJ} represented by a pairwise Lennard-Jones potential with energy ϵ , (ii) an anisotropic interaction contribution with characteristic energy $J(c)$

and proportional to the total number of HBs N_{HB} representing the directional HB interaction H_J , (iii) a cooperative HB interaction contribution H_{coop} with characteristic energy J_σ and (iv) a PV term, where the volume of the system is given by $V = V_0 + N_{HB}v_{HB}$, where V_0 is the volume when the system forms no HBs and v_{HB} is the volume per HB in a system with a fully bonded HB network. Following [4] we choose $\epsilon = 5.8$ kJ/mol, $J_w = 2.9$ kJ/mol, $J_\sigma = 0.29$ kJ/mol, a Van Der Waals diameter $r_0 = 2.9$ Å for the Lennard-Jones potential with $V_0 = Nhr_0^2$, and $v_{HB}/hr_0^2 = 0.5$.

B. Metropolis algorithm

We simulate the system at constant N , P and T following the Metropolis algorithm described in [4]. We accept trial moves with a probability:

$$\hat{P} = \min(1, \exp[-\beta(\Delta H - T\Delta S)]) \quad (6)$$

where

$$\Delta H \equiv H^{trial} - H^{current},$$

$$H \equiv H_{LJ} + H_{HB} + H_{coop} + PV \quad (7)$$

and

$$\Delta S \equiv -Nk_B \ln\left(\frac{V^{trial}}{V^{current}}\right).$$

P and T have units $[P] = \epsilon/hr_0^2$ and $[T] = \epsilon/k_B$. Diffusion is calculated as in ref. [4], being r_o the internal unit for length and rescaling the Monte Carlo time in a T -dependent way to get real time units as explained in ref. [8].

III. RESULTS

We simulate the system with $M = 2500$ and $N = 1875$ (75% of cells occupied). For each simulation we equilibrate for 0.14 ms, and produce data for 7.8 ms.

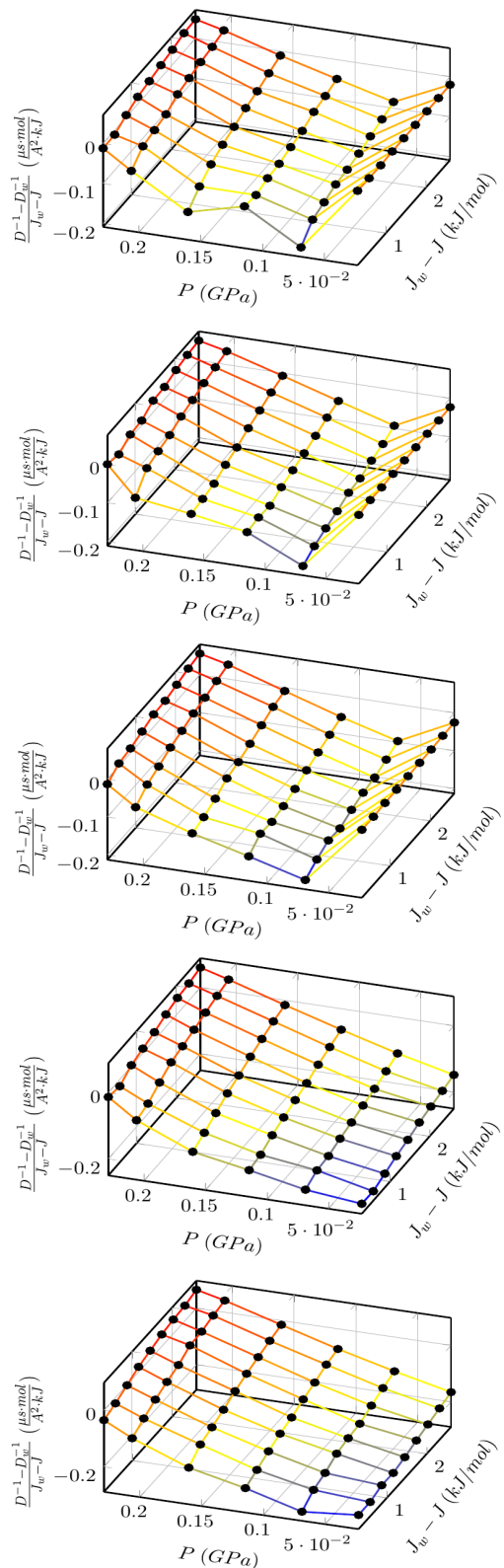


Figure 3: From bottom to top $T=558, 593, 628, 663$ and 698 K. We observe the linear relation predicted from our hypothesis $c \propto \sqrt{J_w - J}$ along the isobaric lines. Also, we observe that for $T=558, 593$ and 628 K, reducing P along iso- $(J_w - J)$ lines, there is a minimum in $(D^{-1} - D_w^{-1})/(J_w - J)$ at T and P that coincide with diffusion minima T and P calculated in ref. [4].

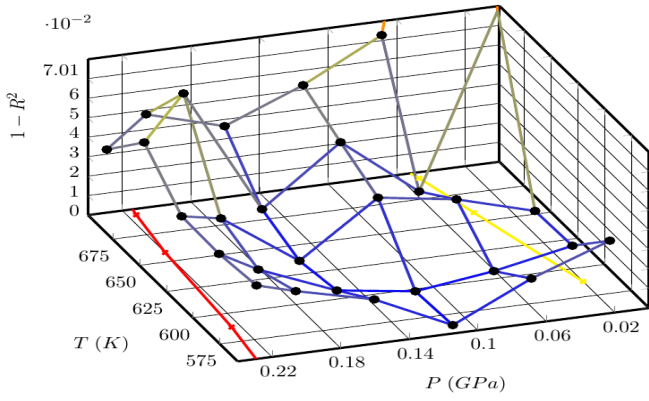


Figure 4: $1 - R^2$ parameter (with R^2 the lineal correlation coefficient) in the P-T plane for the $(D^{-1} - D_w^{-1})/(J_w - J)$ vs. $(J_w - J)$ linear regressions calculated from the first scanning; T=558, 593, 628, 663, 698K; and P=22.9, 68.7, 114.5, 160.3, 206.1, 229 MPa. Also, diffusion minima (yellow line) and maxima (red line) calculated in ref. [4] have been plotted.

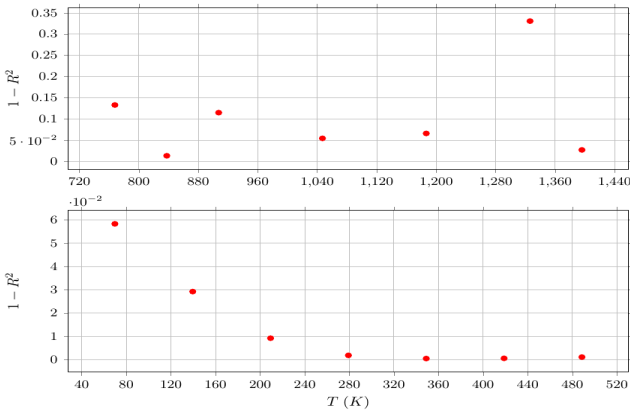


Figure 5: $1 - R^2$ parameter (with R^2 the lineal correlation coefficient) vs. T for the $(D^{-1} - D_w^{-1})/(J_w - J)$ vs. $(J_w - J)$ linear regressions at P=114.5 MPa, $T < 558$ K (bottom) and $T > 698$ K (top).

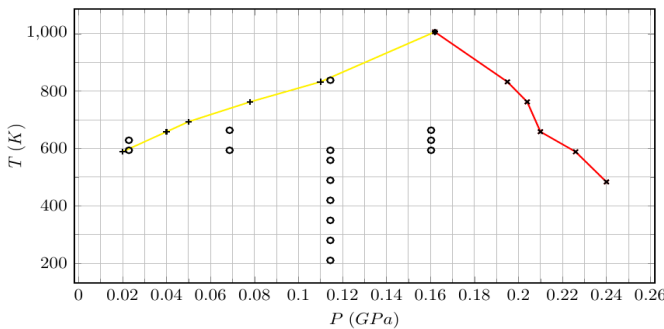


Figure 6: P-T plane with the diffusion maxima (red) and minima (yellow) lines. Points on which $(D^{-1} - D_w^{-1})/(J_w - J)$ vs. $(J_w - J)$ linear regression gives $1 - R^2 < 0.02$ have been plotted (circles).

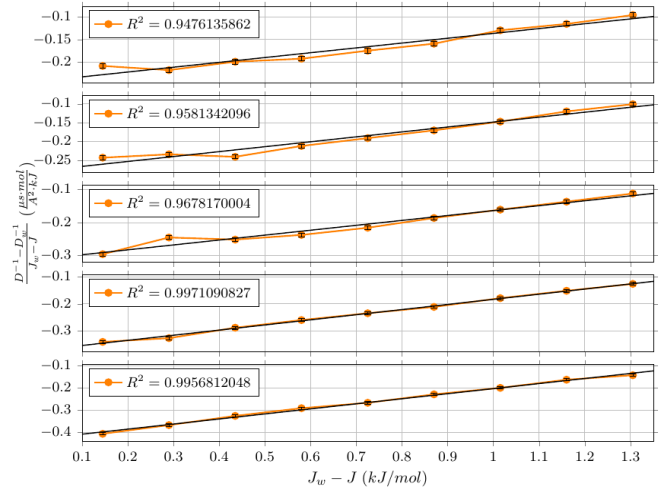


Figure 7: Linear regressions calculated on the $(D^{-1} - D_w^{-1})/(J_w - J)$ vs. $(J_w - J)$ graphic representation for P=114.5 MPa and, from bottom to top, T=558, 593, 628, 663 and 698 K. Error bars have been calculated through standard deviation from various measures of the diffusion. The linear determination coefficient for the linear regressions (R^2) is shown.

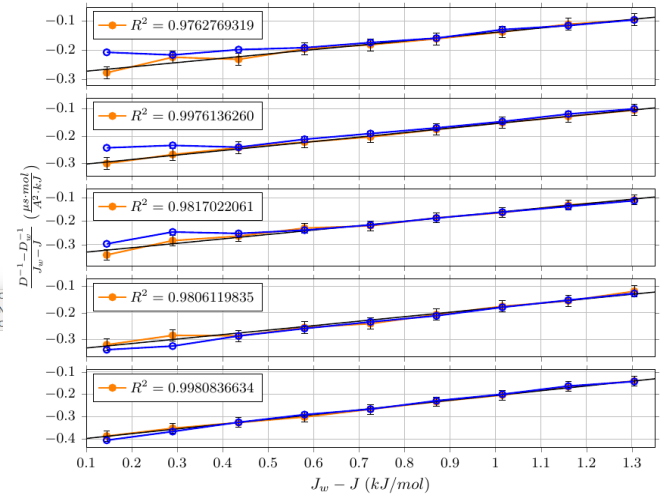


Figure 8: Linear regressions calculated on the $(D^{-1} - D_w^{-1})/(J_w - J)$ vs. $(J_w - J)$ for $J_\sigma = 0$ (orange circles, black regression line) along with the same data for $J_\sigma = 0.29$ kJ/mol (blue circles). P=114.5 MPa and, from bottom to top, T=558, 593, 628, 663 and 698 K. Error bars have been calculated through standard deviation from various measures of the diffusion. The linear determination coefficient for the linear regressions (R^2) is shown.

We have made an initial scanning with T=558, 593, 628, 663 and 698 K; P=22.9, 68.7, 114.5, 160.3, 206.1 and 229 MPa and J=2.61, 2.32, 2.03, 1.74, 1.45, 1.16, 0.87, 0.58 and 0.29 kJ/mol. Results from these simulations can be seen in fig. 3. For every $\frac{D^{-1} - D_w^{-1}}{J_w - J}$ vs. $J_w - J$ series for a given T and P, there has been adjusted a linear regression, as it can be seen in fig. 7. We observe the following:

- Linear regressions fit better for P approximately below $P=206$ MPa and above $P=68$ MPa.
- For a given P in the range $P=68-206$ MPa, linear regressions fit better for temperatures around $T=593$ K. The range of goodness in T is wider around $P=114$ MPa and narrower when we get closer to the extrema $P=68$ MPa or $P=206$ MPa.
- The validity region is approximately within the diffusion anomaly region calculated in [4].

In order to appreciate better in which regions linear regressions fit better to data, $1 - R^2$ parameter has been plotted in the P - T plane (fig. 4, with R^2 being the linear determination coefficient).

To complete our data, we have run simulations at higher and lower T for the fixed central $P=114.5$ MPa, to see the extent of our hypothesis validity in the T range. For those points with low T ($T < 558$ K), equilibration time has been 4 times bigger to compensate the slow equilibration. Results have been analysed in the same way as those from initial scanning, and $1 - R^2$ vs. T has been plotted in fig. 5. For low T we see that there exists a clear minimum around $T=275$ K, below which our hypothesis is not obeyed. For high T we see that above $T=700$ K our hypothesis is not satisfied at all: indeed, the hypothesis is obeyed below $T=698$ K, as it can be seen in fig. 4.

Finally, we performed simulations setting the many body interaction parameter $J_\sigma = 0$. Because in our hypothesis $c > 0$ affects only the directional interaction $J(c)$, and because we find that the Jones-Dole relation holds better at $k_B T \gg J_\sigma$, we expect that setting $J_\sigma = 0$ should have a minor effect on our results. In order to compare its importance, we plot the results along with the original results for $J_\sigma = 0.29$ kJ/mol, both for $P=114.5$ MPa, in fig. 8. We observe almost no appreciable change when we set $J_\sigma = 0$, in agreement with the observations in [4] for the diffusion anomaly.

IV. CONCLUSIONS

Our Monte Carlo simulations for the many-body water monolayer at low ionic concentration c , under the hypothesis that for $c > 0$ the directional component of the HB interaction decreases in a quadratic way, show that that we can recover the empirical Jones-Dole relation, written in terms of diffusion constants, in approximate ranges $P \in [68, 206]$ MPa and $T \in [275, 698]$ K. It is interesting to note that this region is approximately inside the diffusion anomaly region calculated in [4] (see fig. 6).

This observation can be rationalized as follows. The diffusion anomaly region corresponds to a region where the diffusion of water is more sensible to changes in the HB network. Hence it is reasonable to expect that the same region will be also where the diffusion is more easily affected by the addition of ions, making the mean field hypothesis $J(c)$ more realistic.

In this work we considered decreasing J (structure breakers). However, it is worth noting that the same kind of simulations could be made for increasing J (structure makers). In this case J_w would be a minima and the same previous reasoning could be used by changing sign for the quadratic term in eq. (3).

Finally we observe that, as a consequence of our assumption eq. (3) about how the ion concentration affects the hydrogen bond energy without any direct effect for the many-body component of the HB interaction, we find that the Jones-Dole relation holds also if water would have no cooperative interaction.

V. ACKNOWLEDGMENTS

Thanks to Francisco de los Santos for his helpful comments and assistance with the use of the Monte Carlo code he provided for this work.

Also thanks to Giancarlo Franzese for his helpful comments and supervision of this work.

-
- [1] Bernard Cabane, Rodolphe Vuilleumier. The physics of liquid water. Comptes Rendus Geoscience, Elsevier Masson, 2005, 337, pp.159. <hal - 00015954 >
- [2] http://www1.lsbu.ac.uk/water/physical_anomalies.html (Accessed May 29, 2016)
- [3] P. A. Netz *et al.* Translational and rotational diffusion in stretched water. Journal of Molecular Liquids 101 (2002): 159-168.
- [4] G. Franzese, F. J. de los Santos. Understanding diffusion and density anomaly in a coarse-grained model for water confined between hydrophobic walls. J. Phys. Chem. B 2011, 115, 14311-14320
- [5] F. J. de los Santos, G. Franzese. Relations between the diffusion anomaly and cooperative rearranging regions in a hydrophobically nanoconfined water monolayer. Phys. Rev. E 85, 010602(R) (2012)
- [6] T. Corridoni *et al.* Viscosity of Aqueous Solutions and Local Microscopic Structure. J. Phys. Chem. B 2011, 115, 14008-14013
- [7] Y. Yao *et al.* Communication: Modeling of concentration dependent water diffusivity in ionic solutions: Role of intermolecular charge transfer. J. Chem. Phys. 143, 241101 (2015); doi: 10.1063/1.4938083
- [8] M. G. Mazza *et al.* More than one dynamic crossover in protein hydration water. PNAS (2011) vol. 108 no. 50 19873-19878